frontiers in Physics

ORIGINAL RESEARCH
published: 11 December 2020
doi: 10.3389/fphy.2020.609926

# Spreading Kinetics of Herschel-Bulkley Fluids Over Solid Substrates

*Jie Zhang*[1,2]*, *Hai Gu*[1,2], *Jianhua Sun*[1], *Bin Li*[1,2], *Jie Jiang*[1,2] and *Weiwei Wu*[3]

[1]School of Mechanical Engineering, Nantong Institute of Technology, Nantong, China, [2]Jiangsu Key Laboratory of 3D Printing Equipment and Application Technology, Nantong, China, [3]School of Mechanical Engineering, Yangzhou University, Yangzhou, China

The spreading kinetics of Herschel-Bulkley fluids on horizontal solid substrates were theoretically studied. The equations of film thickness were derived in both gravitational and capillary regimes. The dynamic contact angle for the capillary regime was also derived. Finally, a limiting result for the case of $\tau_0 = 0$ was obtained, which was compared with the known solution for validation. The results show that the yield behavior of the fluids had a significant impact on the spreading kinetics in both cases. Only when stress was larger than the yield stress, would substantial flow occur. The spreading zone was divided into two parts by the yield surface: sheared zone and yield zone, which was completely different from common Newtonian fluids or power-law fluids. The thickness of the yield zone mainly depended on yield stress and pressure gradient along the *z*-direction. According to the final evolution, both the film thickness and dynamic contact angle were affected not only by the power-law index but also by the yield behavior.

**Keywords: spreading, Herschel-Bulkley, film thickness, dynamic contact angle, non-newtonian**

OPEN ACCESS

***Edited by:***
*Nuno A. M. Araújo,*
*University of Lisbon, Portugal*

***Reviewed by:***
*Shahin Rouhani,*
*Sharif University of Technology, Iran*
*Martin Kröger,*
*ETH Zürich, Switzerland*

***Correspondence:**
*Jie Zhang*
*zhangjienit@163.com*

***Specialty section:***
*This article was submitted to Mathematical and Statistical Physics, a section of the journal Frontiers in Physics*

***Received:*** *24 September 2020*
***Accepted:*** *17 November 2020*
***Published:*** *11 December 2020*

***Citation:***
*Zhang J, Gu H, Sun J, Li B, Jiang J and Wu W (2020) Spreading Kinetics of Herschel-Bulkley Fluids Over Solid Substrates. Front. Phys. 8:609926. doi: 10.3389/fphy.2020.609926*

## INTRODUCTION

Many studies have addressed the spreading of Newtonian and power-law fluids over solid surfaces by experiments, simulations, and theories [1–7]. For Newtonian fluids, Tanner law is considered to be the classic theory [3]. For power-law fluids, Starov built a hydrodynamic model for the spreading of a complete wetting case [4]. Wang experimentally investigated both complete wetting and partial wetting cases of spreading, which agreed with the theory proposed by Starov [5-6]. Carré and Eustach proposed a simplified theoretical analysis and experimentally observed the drop shape [7].

Besides power-law fluids, Bingham and Herschel-Bulkley fluids also belong to the common non-Newtonian type, which present yielding behavior. For Bingham fluids, the spreading dynamics both in impact and spin-coating cases have been analyzed in detail. In the impact case, the results indicated that the film shape mainly depends on initial yield stress, power-law index, and the impact force [8–13]. In the spin-coating case, the analysis showed that film thickness is not homogeneous, the yield behavior, power-law index, and the centrifugal force are the key factors on spreading dynamics [14–17].

Because of the complex rheological model of Herschel-Bulkley fluids, a minority of theories of complete wetting have been proposed. In this paper, we will theoretically analyze the spreading of Heschel–Bulkley fluids in a complete wetting case based on some proper assumptions. We begins with the simple spreading schematic of Newtonian fluids and the Navier–Stokes equation. According

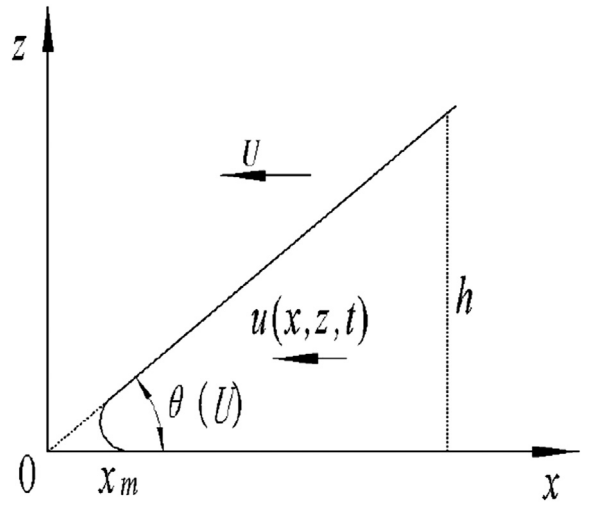


**FIGURE 1 |** Spreading flow schematic figure of Newtonian fluids and power-law fluids.

to the analytical approach of the spreading of power-law fluids, the film thickness equations are derived in both gravitational and capillary regimes and the dynamic contact angle is also discussed.

## ASSUMPTIONS

To simplify the problem, the following assumptions are made [18, 19]. 1) The spreading process belongs to the complete wetting case. 2) The fluids are incompressible, which will ensure the Navier-Stokes equation is workable. 3) The gas viscosity is ignored. 4) The film is much thinner than the horizontal length, so the flow can be converted into 2D. 5) The Reynolds number is small enough to ignore inertial influence. And 6) complete wetting is applied here to ensure a small contact angle.

## THEORY

### The Constitutive Model of Herschel-Bulkley Fluids

The constitutive model of Herschel-Bulkley fluids is similar to Bingham fluids or power-law fluids. The specific constitutive equation is given as follows:

$$\begin{cases} \tau = \tau_0 + k\dot{\gamma}^n, & |\tau| > \tau_0 \\ \dot{\gamma} = 0, & |\tau| \le \tau_0 \end{cases} \tag{1}$$

where $\tau$ is shear stress, $k$ is viscosity coefficient,$\dot{\gamma}$is the shear rate, $n$ is the power-law index, and $\tau_0$ is the initial yield stress.

### Thin Film Equation

The spreading schematic of the advancing system of Newtonian or power-law fluids is shown in **Figure 1**. The derivation of the Herschel-Bulkley case was also started in **Figure 1**. In **Figure 1**, $u$ is the horizontal velocity of the fluid, which is affected by time $t$ and position $x$, $z$. $U$ is the framing moving velocity of the contact line, $\theta(U)$ is the dynamic contact angle, and $h$ is the height of film thickness of any position $x$.

With the proposed assumption **(3)**, the pressure along the $z$-direction will meet the following equation.

$$\frac{\partial p}{\partial z} = -\rho g \tag{2}$$

Applying the Young-Laplace equation to the free surface ($z = h$), there is

$$p = p_G + \sigma\left(\frac{1}{R_1} + \frac{1}{R_2}\right) \approx p_G - \sigma\frac{\partial^2 h}{\partial x^2} \tag{3}$$

where $p_G$ represents the atmospheric pressure and $\sigma$ is surface tension.

Integrating **Eq. (2)** with respect to the boundary condition listed in **Eq. (3)**, the pressure can be further calculated as

$$p = \rho g\,(h - z) + p_G - \sigma\frac{\partial^2 h}{\partial x^2} \tag{4}$$

When $z = 0$, the stress on the horizontal substrate can be obtained from **Eq. (4)** as

$$\tau_s = p|_{z=0} = \rho g h + p_G - \sigma\frac{\partial^2 h}{\partial x^2} \tag{5}$$

Consequently, when the initial yield stress $\tau_0$ is larger than $\tau_s$, substantial flow will not occur. Thus the approximate condition for substantial flow is

$$|\tau_0| < \rho g h + p_G - \sigma\frac{\partial^2 h}{\partial x^2} \tag{6}$$

Substantial flow will be discussed below. Owing to the initial yield stress, there must be a yield surface at $z = h_0$. Thus the spreading zone will be divided into two zones, the significant

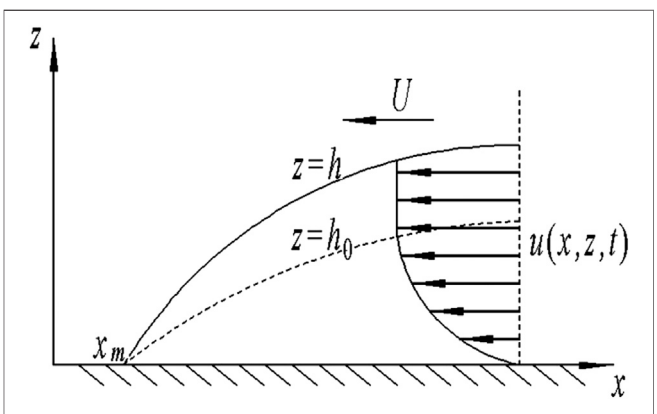


**FIGURE 2 |** The actual spreading flow schematic figure of Herschel-Bulkley fluids.

shear exists only below the yield surface. The shear rate is zero at or above the yield surface. The viewpoint is consistent with the spreading of Bingham fluids proposed by Liu [20]. Therefore, the actual flow schematic of the advancing systems of Herschel-Bulkley fluids is shown in **Figure 2**. The dashed line separates the zone into sheared and yield zones respectively. The schematic figure is completely different from the Newtonian or power-law case.

For the Navier–Stokes equation, it can be written as

$$\frac{\partial p}{\partial x} = \frac{\partial}{\partial z}\left(\mu \frac{\partial u}{\partial z}\right) \tag{7}$$

where $p$ is the pressure and $x$ is the distance of one point from the $z$-axis. According to **Eq. (1)**, when the stress is larger than the yield initial stress, the viscosity can be expressed as

$$\mu = \frac{\tau_0}{|\partial u/\partial z|} + k\left|\frac{\partial u}{\partial z}\right|^{n-1} \tag{8}$$

Substituting **Eq. (8)** into **Eq. (7)**, there is

$$\frac{\partial p}{\partial x} = \frac{\partial}{\partial z}\left[\left(\frac{\tau_0}{|\partial u/\partial z|} + k\left|\frac{\partial u}{\partial z}\right|^{n-1}\right)\frac{\partial u}{\partial z}\right] \tag{9}$$

Based on the boundary condition of no shear at the yield surface ($h(x) = h_0$, $\partial u/\partial z = 0$), integrating **Eq. (9)** with respect to $z$ and the following equation can be acquired.

$$\frac{\partial u}{\partial z} = sign\left(-\frac{\partial p}{\partial x}\right)\left[\left|-\frac{1}{k}\frac{\partial p}{\partial x}\right|(h_0 - z)\right]^{\frac{1}{n}} \tag{10}$$

With the boundary condition of no-slip at the solid surface ($z = 0$, $u = 0$), the expression of $u$ can be obtained by integrating **Eq. (10)**.

$$u = \frac{n}{n+1}\left(\frac{1}{k}\right)^{\frac{1}{n}} sign\left(-\frac{\partial p}{\partial x}\right)\cdot\left|-\frac{\partial p}{\partial x}\right|^{\frac{1}{n}}\left[h_0^{\frac{n+1}{n}} - (h_0 - z)^{\frac{n+1}{n}}\right] \tag{11}$$

**Equation (11)** shows that the maximum velocity $u_p$ occurs at the yield surface $z = h_0$ that can be obtained as

$$u_p = \frac{n}{n+1} sign\left(\sigma\frac{\partial^3 h}{\partial x^3} - \rho g\frac{\partial h}{\partial x}\right)\cdot\left(\frac{1}{k}\right)^{\frac{1}{n}}\left(\sigma\frac{\partial^3 h}{\partial x^3} - \rho g\frac{\partial h}{\partial x}\right)^{\frac{1}{n}} h_0^{\frac{n+1}{n}} \tag{12}$$

When $z > h_0$, the velocity is still equal to the maximum velocity $u_p$. According to mass conservation, there is

$$\frac{\partial h}{\partial t} + \frac{\partial q}{\partial x} = 0 \tag{13}$$

where $q$ is the flow of fluids.

For Herschel-Bulkley fluids, $q$ is made up of two parts as

$$q = \int_0^{h_0} u dz + u_p(h - h_0) \tag{14}$$

The first term of the right side represents the shear zone below the yield surface and its detailed expression is

$$\int_0^{h_0} u dz = \frac{n}{2n+1}\text{sign}\left(\sigma\frac{\partial^3 h}{\partial x^3} - \rho g\frac{\partial h}{\partial x}\right)\left(\frac{1}{k}\right)^{\frac{1}{n}}\left(\sigma\frac{\partial^3 h}{\partial x^3} - \rho g\frac{\partial h}{\partial x}\right)^{\frac{1}{n}} h_0^{\frac{2n+1}{n}} \tag{15}$$

Then the flow $q$ will be acquired as follows:

$$q = \frac{n}{2n+1}\text{sign}\left(\sigma\frac{\partial^3 h}{\partial x^3} - \rho g\frac{\partial h}{\partial x}\right)\left(\frac{1}{k}\right)^{\frac{1}{n}}\left(\sigma\frac{\partial^3 h}{\partial x^3} - \rho g\frac{\partial h}{\partial x}\right)^{\frac{1}{n}} h_0^{\frac{2n+1}{n}} + \frac{n}{n+1}\text{sign}\left(\sigma\frac{\partial^3 h}{\partial x^3} - \rho g\frac{\partial h}{\partial x}\right)\left(\frac{1}{k}\right)^{\frac{1}{n}}\left(\sigma\frac{\partial^3 h}{\partial x^3} - \rho g\frac{\partial h}{\partial x}\right)^{\frac{1}{n}} h_0^{\frac{n+1}{n}}(h - h_0) \tag{16}$$

In **Fig. 2**, the velocity along the $x$-direction is parabolic, which can also be explained by **Eqs. (11)–(12)**. When it refers to the velocity, the case here is similar to classical Poiseuille flow. Both of them are driven by the pressure gradient, and they have the same initial and boundary conditions, thus the relationship between $h$ and $h_0$ can be obtained based on our previous work [21–22] as

$$h_0 = h - \frac{\tau_0}{|\partial p/\partial z|} = h - \frac{\tau_0}{\rho g} \tag{17}$$

Substituting **Eq. (17)** into **Eq. (16)**, a new formula of flow $q$ is generated as

$$q = \frac{n}{2n+1}\text{sign}\left(\sigma\frac{\partial^3 h}{\partial x^3} - \rho g\frac{\partial h}{\partial x}\right)\left(\frac{1}{k}\right)^{\frac{1}{n}}\left(\sigma\frac{\partial^3 h}{\partial x^3} - \rho g\frac{\partial h}{\partial x}\right)^{\frac{1}{n}} h_0^{\frac{2n+1}{n}} + \frac{n}{n+1}\text{sign}\left(\sigma\frac{\partial^3 h}{\partial x^3} - \rho g\frac{\partial h}{\partial x}\right)\left(\frac{1}{k}\right)^{\frac{1}{n}}\left(\sigma\frac{\partial^3 h}{\partial x^3} - \rho g\frac{\partial h}{\partial x}\right)^{\frac{1}{n}} h_0^{\frac{n+1}{n}}\frac{\tau_0}{\rho g} \tag{18}$$

Finally, substituting **Eq. (18)** into **Eq. (13)**, the following equation is obtained as

$$\frac{\partial h}{\partial t} + \frac{n}{2n+1}\text{sign}\left(\sigma\frac{\partial^3 h}{\partial x^3} - \rho g\frac{\partial h}{\partial x}\right)\left(\frac{1}{k}\right)^{\frac{1}{n}}\frac{\partial}{\partial x}\left[\left|\sigma\frac{\partial^3 h}{\partial x^3} - \rho g\frac{\partial h}{\partial x}\right|^{\frac{1}{n}} h_0^{\frac{2n+1}{n}}\right] + \frac{n}{n+1}\text{sign}\left(\sigma\frac{\partial^3 h}{\partial x^3} - \rho g\frac{\partial h}{\partial x}\right)\left(\frac{1}{k}\right)^{\frac{1}{n}}\frac{\partial}{\partial x}\left[\left|\sigma\frac{\partial^3 h}{\partial x^3} - \rho g\frac{\partial h}{\partial x}\right|^{\frac{1}{n}} h_0^{\frac{n+1}{n}}\frac{\tau_0}{\rho g}\right] = 0 \tag{19}$$

According to **Eq. (16)**, the pressure mainly depends on the gravity and capillary forces. In the following part, two limiting regimes will be considered further. One is only the gravitational regime taken into consideration by ignoring the capillary force, $\rho g R^2 >> \sigma$. The other is only the capillary force regime considered, ignoring the gravity, $\sigma >> \rho g R^2$.

## Gravitational Spreading Regime

The capillary force is ignored here, so **Eq. (19)** can be simplified into the following equation.

$$\frac{\partial h}{\partial t}+\mathrm{sign}\left(-\rho g\frac{\partial h}{\partial x}\right)\left(\frac{\rho g}{k}\right)^{\frac{1}{n}}\frac{\partial}{\partial x}\left[\left|-\frac{\partial h}{\partial x}\right|^{\frac{1}{n}}h_0^{\frac{n+1}{n}}\left(\frac{n}{2n+1}h_0+\frac{n}{n+1}\frac{\tau_0}{\rho g}\right)\right]=0 \tag{20}$$

When the contact line moves at velocity $U$, the above equation can be converted into the following form by introducing a new variable $\xi = x - Ut$.

$$-U\frac{dh_0}{d\xi}+\left(\frac{\rho g}{k}\right)^{\frac{1}{n}}\frac{d}{d\xi}\left[\left(\frac{dh_0}{d\xi}\right)^{\frac{1}{n}}h_0^{\frac{n+1}{n}}\left(\frac{n}{2n+1}h_0+\frac{n}{n+1}\frac{\tau_0}{\rho g}\right)\right]=0 \tag{21}$$

Integrating the above equation with respect to $\xi$, there is

$$U^n=\left(\frac{n}{2n+1}\right)^n\frac{\rho g}{k}\frac{dh_0}{d\xi}h_0\left(h_0+\frac{2n+1}{n+1}\frac{\tau_0}{\rho g}\right)^n \tag{22}$$

With the boundary condition: $\xi = 0$, $h = 0$, **Eq. (22)** can be solved as

$$\begin{aligned}&\frac{1}{n+2}\left[\left(h+\frac{n}{n+1}\frac{\tau_0}{\rho g}\right)^{n+2}-\left(\frac{n}{n+1}\frac{\tau_0}{\rho g}\right)^{n+2}\right]-\frac{2n+1}{(n+1)^2}\\&\cdot\frac{\tau_0}{\rho g}\left[\left(h+\frac{n}{n+1}\frac{\tau_0}{\rho g}\right)^{n+1}-\left(\frac{n}{n+1}\frac{\tau_0}{\rho g}\right)^{n+1}\right]\\&=\left(U\frac{2n+1}{n}\right)^n\frac{k}{\rho g}\xi\end{aligned} \tag{23}$$

**Equation (23)** addresses the fact that film thickness in capillary spreading is determined by initial yield stress $\tau_0$ and power index $n$.

## Capillary Spreading Regime

In the condition, the gravitational action is ignored, then **Eq. (19)** can be simplified as follows

$$\frac{\partial h}{\partial t}+\mathrm{sign}\left(\sigma\frac{\partial^3 h}{\partial x^3}\right)\left(\frac{1}{k}\right)^{\frac{1}{n}}\frac{\partial}{\partial x}\left\{\left(\sigma\frac{\partial^3 h}{\partial x^3}\right)^{\frac{1}{n}}h_0^{\frac{n+1}{n}}\left[\frac{n}{2n+1}h_0+\frac{n}{n+1}\frac{\tau_0}{\rho g}\right]\right\}=0 \tag{24}$$

Introducing the above variable $\xi$ and $h_0$ into **Eq. (24)**,

$$\begin{aligned}&-U\frac{dh_0}{d\xi}+\mathrm{sign}\left(\sigma\frac{d^3h_0}{d\xi^3}\right)\left(\frac{1}{k}\right)^{\frac{1}{n}}\\&\frac{d}{d\xi}\left\{\left(\sigma\frac{\partial^3 h_0}{\partial\xi^3}\right)^{\frac{1}{n}}h_0^{\frac{n+1}{n}}\left[\frac{n}{2n+1}h_0+\frac{n}{n+1}\frac{\tau_0}{\rho g}\right]\right\}=0\end{aligned} \tag{25}$$

Integrating the above equation with respect to $\xi$,

$$-U+\frac{n}{2n+1}\left(\frac{1}{k}\right)^{\frac{1}{n}}\left(\sigma\frac{d^3h_0}{d\xi^3}\right)^{\frac{1}{n}}h_0^{\frac{1}{n}}\left[h_0+\frac{2n+1}{n+1}\frac{\tau_0}{\rho g}\right]=0 \tag{26}$$

Then it is supposed that $\frac{\tau_0}{\rho g}=\lambda h_0$, so **Eq. (26)** can be translated into

$$U^n=\left[\frac{n}{2n+1}\cdot\frac{(2\lambda+1)n+(\lambda+1)}{n+1}\right]^n\frac{\sigma}{k}\frac{d^3h_0}{d\xi^3}h_0^{n+1} \tag{27}$$

With the boundary condition: $\xi = 0$, $h = 0$, **Eq. (27)** can be solved as

$$h_0^{n+2}=\frac{k}{\sigma}\left[U\frac{(2n+1)(n+1)}{n(n(2\lambda+1)+(\lambda+1))}\right]^n\left[\frac{(n+2)^3}{3(2n+1)|n-1|}\right]\xi^3\quad(n\neq1) \tag{28}$$

Further, the film thickness equation can be obtained by replacing $h_0$,

$$\left(h-\frac{\tau_0}{\rho g}\right)^{n+2}=\frac{k}{\sigma}\left[U\frac{(2n+1)(n+1)}{n(n(2\lambda+1)+(\lambda+1))}\right]^n\left[\frac{(n+2)^3}{3(2n+1)|n-1|}\right]\xi^3\quad(n\neq1) \tag{29}$$

Based on **Eq. (17)**, the variable $\lambda$ can be calculated as

$$\lambda=\frac{\tau_0/\rho g}{h-\tau_0/\rho g} \tag{30}$$

In this way, the equation of film thickness $h$ can be obtained, which depends on the power index $n$ and initial yield stress $\tau_0$.

## Dynamic Contact Angle

The inclination angle at $x = \xi$ can be calculated by differentiating film thickness $h$ as shown in **Eq. (29)** for the capillary spreading regime.

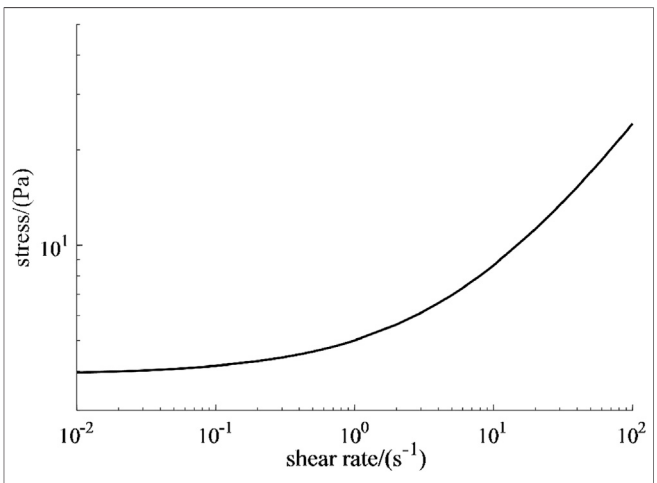


**FIGURE 3 |** The rheological model of Herschel-Bulkley fluids.

$$\tan\theta = \frac{dh}{d\xi} = \frac{\frac{k}{\sigma}U^n\left[\frac{(n+2)^3}{(2n+1)|n-1|}\right]}{(h-\tau_0/\rho g)\left[\frac{n(n+1)h+n^2\tau_0/\rho g}{(2n+1)(n+1)}\right]^{n-1}\left\{(n+2)\left[\frac{n(n+1)h+n^2\tau_0/\rho g}{(2n+1)(n+1)}\right]-\frac{n^2\tau_0/\rho g}{n+1}\right\}}\xi^2 \quad (n\neq 1) \tag{31}$$

In previous studies, many researchers found that the local microscopic contact angle can not be measured directly for boundary conditions. Thus dynamic contact angle $\theta$ is taken as the replacement, which is equal to the inclination angle at $x = x_m$. Furthermore, the dynamic contact angle can be obtained as

$$\theta \approx \tan\theta = \frac{\frac{k}{\sigma}U^n\left[\frac{(n+2)^3}{(2n+1)|n-1|}\right]}{(h-\tau_0/\rho g)\left[\frac{n(n+1)h+n^2\tau_0/\rho g}{(2n+1)(n+1)}\right]^{n-1}\left\{(n+2)\left[\frac{n(n+1)h+n^2\tau_0/\rho g}{(2n+1)(n+1)}\right]-\frac{n^2\tau_0/\rho g}{n+1}\right\}}x_m{}^2 \quad (n\neq 1) \tag{32}$$

To obtain **Eq. (32)**, it is considered that when the angle $\theta$ is small enough, it is approximately equal to sin $\theta$ or tan $\theta$.

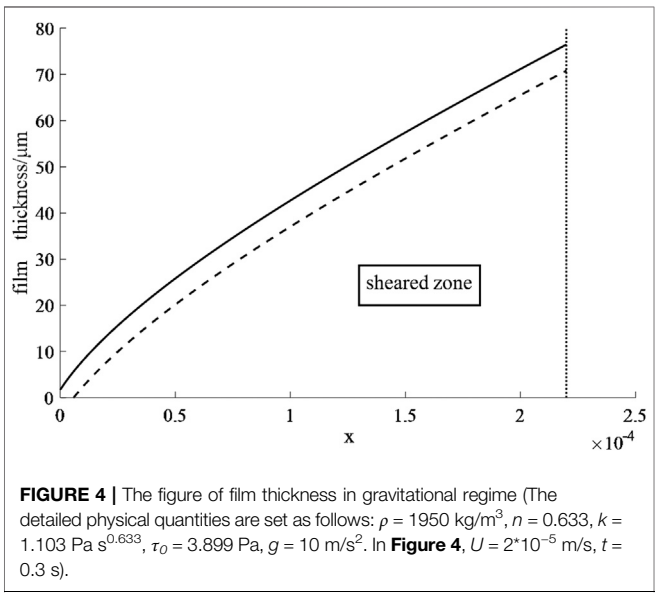


**FIGURE 4 |** The figure of film thickness in gravitational regime (The detailed physical quantities are set as follows: $\rho$ = 1950 kg/m$^3$, $n$ = 0.633, $k$ = 1.103 Pa s$^{0.633}$, $\tau_0$ = 3.899 Pa, $g$ = 10 m/s$^2$. In **Figure 4**, $U$ = 2*10$^{-5}$ m/s, $t$ = 0.3 s).

## EXAMPLE

In a previous study [21, 22], the typical Herschel-Bulkley model was obtained as follows

$$\begin{cases} \tau = 3.899 + 1.103\dot{\gamma}^{0.633}, & \tau_0 \geq 3.899 \\ \dot{\gamma} = 0 \quad , & \tau_0 < 3.899 \end{cases} \tag{33}$$

The rheological figure is shown in **Figure 3**. The model was taken as an example to explain the spreading results.

**Figure 4** gives the film thickness in the gravitational regime. The area below the dashed line is the sheared zone. In Figure 5, the figure of the contact angle vs. the moving velocity at different film thicknesses is presented. It can be found that a thinner film will lead to a smaller contact angle.

## DISCUSSION AND CONCLUSION

The spreading of Herschel-Bulkley fluids over solid substrates for a complete wetting case was theoretically studied here. The film thicknesses in both the gravitational and capillary regimes were derived and the dynamic contact angles were also explored. There was an obvious difference between other kinds of fluids

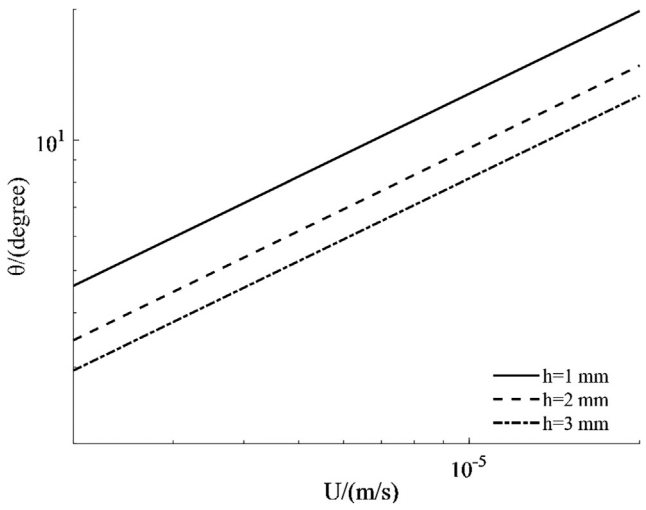


**FIGURE 5 |** The contact angles at different film thicknesses.

(Newtonian fluids and power-law fluids). The flow was dramatically affected by the yield behavior of Herschel-Bulkley fluids. According to the analysis, only when the stress on the substrate was larger than the initial yield stress $\tau_0$, would the flow be appreciable. Even if appreciable flow occurred, the spreading zone was also divided into two zones: one was the shear zone and the other was the yield zone. The dividing surface was named yield surface at $z = h_0$, which does not exist in common fluids such as Newtonian fluids or power-law fluids. In "**Example**" section, the detailed numerical examples are given to explain the results further.

It is noteworthy that when initial yield stress $\tau_0 = 0$, the fluids become power-law fluids. The film thicknesses of the gravitational regime and the capillary regime will be obtained as follows

$$h^{n+2} = (n+2)\frac{k}{\rho g}\left(U\frac{2n+1}{n}\right)^n \xi \tag{34}$$

$$h^{n+2} = \frac{k}{\sigma}\left[U\frac{2n+1}{n}\right]^n \left[\frac{(n+2)^3}{3(2n+1)|n-1|}\right]\xi^3 \quad (n \neq 1) \tag{35}$$

**Equations (34)** and **(35)** represent the gravitational case and the capillary case, respectively. Also, the dynamic contact angle $\theta$ of the capillary regime will be

$$\theta \approx \tan\theta = \frac{\frac{k}{\sigma}U^n\left[\frac{(n+2)^2}{(2n+1)^{1-2n}|n-1|}\right]}{(n+2)n^n h^{n+1}}\xi^2 \qquad (n \neq 1) \tag{36}$$

Substituting **Eq. (35)** into **Eq. (36)**, then the specific equation of the dynamic contact angle can be obtained as

$$\theta^{n+2} = \left(\frac{k}{\sigma}U^n\right)\left[\frac{3^{n+1}(n+2)^{1-n}}{(2n+1)^{1-n}|n-1|n^n}\right]x_m{}^{1-m} \qquad (n \neq 1) \tag{37}$$

It can be found that all of them are in agreement with the results obtained by Wang [5]. Another noticeable feature of the analysis is that some of the equations have a collective limitation $n \neq 1$, which means the theoretical results are not applicable for Bingham fluids, although the fluid corresponds to it when $n = 1$.

## DATA AVAILABILITY STATEMENT

The original contributions presented in the study are included in the article/**Supplementary Material**, further inquiries can be directed to the corresponding author.

## AUTHOR CONTRIBUTIONS

JZ: idea, HG: method, JS: calculation, BL: calculation, JZ: calculation, WW: validation and writing.

## FUNDING

This work was financially supported by the Young and Middle-Aged Scientific Research Backbone Training Project of Nantong Institute of Technology (Grant No. ZQNGG204), the Key University Science Research Project of Jiangsu Province (Grant No. 18KJA460006), the Priority Discipline Construction Program of Jiangsu Province (Grant No. 2016-9), the Top-Notch Academic Programs Project of Jiangsu Higher Education Institutions (Grant No. 2020-9), and the Key R&D plan of Jiangsu Province (Grant No. BE2018010-4).

## SUPPLEMENTARY MATERIAL

The Supplementary Material for this article can be found online at: https://www.frontiersin.org/articles/10.3389/fphy.2020.609926/full#supplementary-material.

## REFERENCES

1. Liang ZP, Wang XD, Lee DJ. Spreading dynamics of power-law fluid droplets. *Phys-Condens Mat* (2009) 21:3543–9. doi:10.1088/0953-8984/21/46/464117
2. Neogi P, Ybarra RM. The absence of a rheological effect on the spreading of small drops. *J Chem Phys* (2001) 115:7811–3. doi:10.1063/1.1415455
3. Tanner LH. The spreading of silicone oil drops on horizontal surfaces. *J Phys D Appl Phys* (1979) 12:1473. doi:10.1088/0022-3727/12/9/009
4. Starov VM, Tyatyushkin AN, Velarde MG. Spreading of non-Newtonian liquids over solid substrates. *J Colloid Interface Sci* (2003) 257:284–90. doi:10.1016/s0021-9797(02)00034-6
5. Zhdanov XD, Lee DJ, Peng XF. Spreading dynamics and dynamic contact angle of non-Newtonian fluids. *Langmuir* (2007) 23:8042–7. doi:10.1021/la0701125
6. Lai XD, Zhang Y, Lee DJ. Spreading of completely wetting or partially wetting power-law fluid on solid surface. *Langmuir* (2007) 23:9258–62. doi:10.1021/la700232y
7. Peng A, Eustache F. Spreading kinetics of shear-thinning fluids in wetting and dewetting modes. *Langmuir* (2000) 16:2936–41. doi:10.1021/la991021d
8. German G, Bertola V. The spreading behaviour of capillary driven yield-stress drops. *Colloid Surf Physicochem Eng Aspect* (2010) 366:18–26. doi:10.1016/j.colsurfa.2010.05.019
9. German G, Bertola V. Impact of shear-thinning and yield-stress drops on solid substrates. *J Phys Condens Matter* (2009) 21:375111. doi:10.1088/0953-8984/21/37/375111
10. Nigen S. Experimental investigation of the impact of an (apparent) yield-stress material. *Atomization Sprays* (2005) 15:103–18. doi:10.1615/atomizspr.v15.i1.60
11. Saïdi A, Martin C, Magnin A. Influence of yield stress on the fluid droplet impact control. *J Non-Newtonian Fluid Mech* (2010) 165:596–606. doi:10.1016/j.jnnfm.2010.02.020
12. Luu L-H, Forterre Y. Drop impact of yield-stress fluids. *J Fluid Mech* (2009) 632:301–27. doi:10.1017/s0022112009007198
13. Kim E, Baek J. Numerical study of the parameters governing the impact dynamics of yield-stress fluid droplets on a solid surface. *J Non-Newtonian Fluid Mech* (2012) 173–174:62–71. doi:10.1016/j.jnnfm.2012.02.005
14. Burgess SL, Wilson SDR. Spin-coating of a viscoplastic material. *Phys Fluids* (1996) 8(9):2291–7. doi:10.1063/1.869016
15. Jenekhe SA, Schuldt SB. Flow and film thickness of Bingham plastic liquids on a rotating disk. *Chem Eng Commun* (1985) 33:135–47.
16. Tabuteau H, Baudez JC, Chateau X. Flow of a yield stress fluid over a rotating surface. *Rheol Acta* (2007) 46:341–55. doi:10.1080/00986448508911165

17. Tsamopoulos JA, Chen ME, Borkar AV. On the spin coating of viscoplastic fluids. *Rheol Acta* (1996) 35:597–615. doi:10.1007/bf00396510
18. Fermigier M, Jenffer P. An experimental investigation of the dynamic contact angle in liquid–liquid systems. *J Colloid Interface Sci* (1991) 146:226–41. doi:10.1016/0021-9797(91)90020-9
19. Chen J-D, Wada N. Edge profiles and dynamic contact angles of a spreading drop. *J Colloid Interface Sci* (1992) 148:207–22. doi:10.1016/0021-9797(92)90129-a
20. Liu KF, Mei CC. Approximate equations for the slow spreading of a thin sheet of Bingham plastic fluid. *Phys Fluids* (1998) 2(1):30–6.
21. Wu W, Huang X, Fang C. An improved MRT-LBM for Herschel-Bulkley fluids with high Reynolds number, *Numer Heat Tr B-Fund* (2017) 72(6):1–12. doi:10.1080/10407790.2017.1409521
22. Wu W, Huang X, Li Y, Fangau C, Jiang X. A modified LBM for non-Newtonian effect of cement paste flow in 3D printing. *Rpj* (2019) 25(1):22–9. doi:10.1108/rpj-06-2017-0124

**Conflict of Interest:** The authors declare that the research was conducted in the absence of any commercial or financial relationships that could be construed as a potential conflict of interest.

# GLOSSARY

## Nomenclature Symbols

$g$ Gravitational acceleration

$h$ The height of film thickness at position $x$

$h_0$ The film thickness of yield surface

$k$ Viscosity coefficient

$n$ The power-law index

$p$ Pressure

$p_G$ Atmospheric pressure

$q$ Flow of fluids

$t$ Time

$u$ Velocity along the $x$-direction

$u_p$ Maximum velocity of $u$

$U$ Frame moving velocity

$x/z$ Values at two directions in the Cartesian coordinate system

$\dot{\gamma}$ Shear rate

$\theta$ Dynamic contact angle

$\lambda$ Variable

$\xi$ Variable, $\xi = x\text{-}Ut$

$\rho$ Density

$\sigma$ Surface tension

$\tau$ Stress

$\tau_0$ Initial yield stress

$\tau_s$ Stress on the substrate